THE JOURNAL OF BIOLOGICAL CHEMISTRY VOL. 287, NO. 31, pp. 26365–26376, July 27, 2012

Structural Features Affecting Trafficking, Processing, and Secretion of *Trypanosoma cruzi* Mucins*[S]

Received for publication, February 21, 2012, and in revised form, June 8, 2012 Published, JBC Papers in Press, June 15, 2012, DOI 10.1074/jbc.M112.354696

Gaspar E. Cánepa[‡1,2], **Andrea C. Mesías**[‡1], **Hai Yu**[§], **Xi Chen**[§], **and Carlos A. Buscaglia**[‡3]

From the [‡]*Instituto de Investigaciones Biotecnológicas "Dr. Rodolfo Ugalde," Av. 25 de Mayo y Francia, Campus UNSAM, San Martín 1650, Buenos Aires, Argentina and the* [§]*Department of Chemistry, University of California, Davis, California 95616*

Background: The surface of *Trypanosoma cruzi* is covered in mucins.
Results: We dissected the role of post-translational modifications on mucin processing.
Conclusion: Glycan elaboration is dependent on the particular mucin product and the developmental stage of the parasite.
Significance: Our findings indicate that GPI-anchors function as forward transport signals along the secretory pathway and support novel roles for mucins in the *T. cruzi*/host interplay.

***Trypanosoma cruzi* is wrapped by a dense coat of mucin-type molecules encoded by complex gene families termed *TcSMUG* and *TcMUC*, which are expressed in the insect- and mammal-dwelling forms of the parasite, respectively. Here, we dissect the contribution of distinct post-translational modifications on the trafficking of these glycoconjugates. *In vivo* tracing and characterization of tagged-variants expressed by transfected epimastigotes indicate that although the N-terminal signal peptide is responsible for targeting TcSMUG products to the endoplasmic reticulum (ER), the glycosyl phosphatidylinositol (GPI)-anchor likely functions as a forward transport signal for their timely progression along the secretory pathway. GPI-minus variants accumulate in the ER, with only a minor fraction being ultimately released to the medium as anchorless products. Secreted products, but not ER-accumulated ones, display several diagnostic features of mature mucin-type molecules including extensive *O*-type glycosylation, Gal*f*-based epitopes recognized by monoclonal antibodies, and terminal Gal*p* residues that become readily sialylated upon addition of parasite *trans*-sialidases. Processing of *N*-glycosylation site(s) is dispensable for the overall TcSMUG mucin-type maturation and secretion. Despite undergoing different *O*-glycosylation elaboration, TcMUC reporters yielded quite similar results, thus indicating that (i) molecular trafficking signals are structurally and functionally conserved between mucin families, and (ii) TcMUC and TcSMUG products are recognized and processed by a distinct repertoire of stage-specific glycosyltransferases. Thus, using the fidelity of a homologous expression system, we have defined some biosynthetic aspects of *T. cruzi* mucins, key molecules involved in parasite protection and virulence.**

Glycosyl phosphatidylinositol (GPI)[4] anchoring is an alternative post-translational method for attaching proteins to the lipid bilayer of eukaryotic cells (1, 2). Proteins destined to be GPI-anchored are translated with a cleavable N-terminal signal peptide (SP) that directs the nascent polypeptide to the endoplasmic reticulum (ER). Immediately after ER translocation, the C-terminal GPI attachment signal is cleaved by a transamidase multi-protein complex that adds a preformed GPI *en bloc* to the ensuing terminal ethanolamine phosphate.

GPI biosynthesis is essential for yeasts (3) and for embryonic development in mammals (4), and GPI-anchored molecules (GPI-AMs) participate in critical biological processes such as cell-cell communication, complement regulation, antigenic presentation and prion pathogenesis (2). Because of their affinity for cholesterol- and sphingolipid-rich domains, GPI-anchors are also involved in the generation of discrete lipid rafts, which may serve as platforms for cell-cell communication, vesicular trafficking, and signal transduction (5). The particular type of association with the cell surface determines that GPI-AMs can be (i) densely packed with minimal perturbation of the underneath plasma membrane, as epitomized in trypanosomes (1), (ii) spontaneously transferred between cells (6), and (iii) secreted into the medium via phospholipase cleavage.

There is a growing body of evidence suggesting that, in addition to their structural role(s), GPI anchors also regulate protein trafficking. In polarized epithelial cells, for instance, GPI anchors play a role in post-Golgi sorting by targeting attached proteins to the apical surface (7). Treatment of cells with inhibitors of ceramide synthase or agents that deplete cholesterol impairs the apical sorting of GPI-AMs, strongly suggesting that this phenomenon relies on the association of GPI-moieties with lipid rafts. On the other hand, it has been demonstrated in a variety of model systems that GPI anchors are key factors in the ER-to-Golgi vesicular transport. Briefly, GPI-AMs are selectively incorporated at the ER exit sites (ERES) in particular COPII-coated, pre-budding complexes in which soluble and

* This investigation received financial support from the UNICEF/UNDP/World Bank/WHO Special Programme for Research and Training in Tropical Diseases (TDR), Agencia Nacional de Promoción Científica y Tecnológica (ANPCyT), Fundación Florencio Fiorini, and UNSAM (to C. A. B.).
[S] This article contains supplemental Figs. S1–S2 and Table S1.
[1] Both authors contributed equally to this work.
[2] Holds a post-doctoral fellowship from the Argentinean Research Council (CONICET).
[3] A career investigator from the Argentinean Research Council (CONICET). To whom correspondence should be addressed: Instituto de Investigaciones Biotecnológicas "Dr. Rodolfo Ugalde," Av. 25 de Mayo y Francia, Campus UNSAM, San Martín 1650, Buenos Aires, Argentina. Tel.: 54-11-4006-1500 int. 2146; Fax: 54-11-4006-1559; E-mail: cbusca@iib.unsam.edu.ar.

[4] The abbreviations used are: GPI, glycosyl phosphatidylinositol; SP, signal peptide; ER, endoplasmic reticulum; ERES, ER exit site; GPI-AM, GPI-anchored molecule; TS, *trans*-sialidase; SA, sialic acid; Gp35/50 mucins, 35–50 kDa mucins coating *T. cruzi* metacyclic trypomastigote and epimastigote forms.

transmembrane cargoes are largely excluded (8, 9). These vesicles are exported to the Golgi apparatus, and from there to their final destination, following distinctive kinetics/routes than the bulk flow. Since GPI-AMs are exclusively luminal and cannot interact directly with the cytosolic COPII coat, they likely use an intermediate transmembrane receptor/adaptor that couples cargo selection based on their membrane anchorage with vesicle coat assembly. Different members of the p24 family, which are abundant type I transmembrane proteins assembled into heteromeric complexes that cycle between the ER and Golgi compartments, are appealing candidates for the formation of this molecular sieve (10–12). The core mechanism of GPI-AM sorting/trafficking along the secretory pathway is conserved across eukaryotes, although variations such as the need for additional molecular players, GPI fatty acid remodeling and/or sphingolipid synthesis, and therefore for the formation of lipid rafts, have been described (13, 14).

GPI-AMs are particularly abundant in the surface coat of pathogenic protozoa such as *Trypanosoma*, *Leishmania*, *Plasmodium*, and *Toxoplasma* (1, 15, 16). Acting at the interface with the infected host, protozoan GPI-AMs are differentially though ideally suited to fulfil a dual purpose: to provide protection against the insect vector- or vertebrate host-derived defense mechanisms and to ensure the targeting and invasion of specific cells/tissues. Their key role is further underscored by the staggering number of encoding genes, which usually show extensive sequence polymorphisms and/or stage-specific expression (16–18).

Trypanosoma cruzi is the etiological agent of Chagas disease, the most important parasitic disease in Latin America with an infection toll estimated in 8–11 million people (19). Mucin-type molecules are prevalent and distinctive GPI-AMs of its surface coat, evenly distributed over the entire plasma membrane (cell body, flagellum, and flagellar pocket) of different developmental forms. They bear short *O*-linked oligosaccharide chains that represent up to 60% of the total mass of the glycoprotein, thus conferring them a strong hydrophilic character (16). In addition to the initial αGlcNAc, which is attached to the hydroxyl group of Ser/Thr residues by a Golgi-resident glycosyltransferase (20), *O*-glycans in *T. cruzi* mucins are elongated with up to 5 Gal residues in either pyranosic (Gal*p*) or furanosic (Gal*f*) configuration and in a variety of linkages (21). Once exported to the parasite surface, terminal Gal*p* residues can be further decorated with sialic acid (SA) residues in a reaction catalyzed by parasite-encoded *trans*-sialidases (TS) (22). Despite being unable to synthesize SA *de novo*, sialylation of surface mucins is essential to evade immune mechanisms and to propagate within the mammalian host (16). *T. cruzi* mucins have also been shown to (i) form a macromolecular diffusion barrier that protects parasites against proteases/glycosidases, (ii) contribute to parasite invasion of mammalian cells (23, 24), and (iii) subvert different pathways of the vertebrate immune system (25, 26).

The *T. cruzi* genome comprises a large repository of mucin genes, which were grouped into two gene families, *TcSMUG* and *TcMUC*, based on sequence comparisons (16, 27). Cumulative expression data indicate that this dichotomy has a functional correlate, as transition between developmental forms leads to the expression of different, non-overlapping set of mucin genes (22, 28, 29). Briefly, TcSMUG products, and particularly the TcSMUG S ones, provide the backbone for the 35–50 kDa mucins (also known as Gp35/50 mucins) expressed on the surface of developmental forms found within the triatomines, *i.e.* replicative epimastigotes and infectious metacyclic trypomastigotes. In contrast, TcMUC products, and particularly those belonging to the TcMUC II subgroup, code for the peptide scaffolds of 60–200 kDa mucins restricted to the surface coat of bloodstream trypomastigotes. Despite their complexity and variations in amino acid sequence, TcMUC and TcSMUG deduced products share a common structure made up of three main domains: one N-terminal SP, one central region showing highly biased amino acid composition, in which Thr, Ser, Pro, Gly, and Ala residues together might add up to 60–80% of the total count whereas Cys and aromatic residues are largely underrepresented, and a C-terminal GPI attachment signal. The central region, which is the only one present in the mature, surface-associated products, bears multiple *O*-glycan addition sites and, in some cases, also a few (1 to 3) *N*-glycosylation consensus signals.

We recently showed that tagged versions of TcSMUG and TcMUC II products are displayed on the surface of transfected parasites as mucin-type GPI-AMs (30).[5] Here, we used a similar homologous expression system to study the importance of different structural features, and particularly GPI anchors, in the trafficking, maturation, and secretion of *T. cruzi* mucins.

EXPERIMENTAL PROCEDURES

Parasites—Epimastigotes from the Adriana stock, typed within the TcI evolutionary lineage (30) were used. Parasites were grown at 28 °C in brain-heart tryptose (BHT) medium supplemented with 10% heat-inactivated fetal bovine serum (FBS) and antibiotics (31, 32).

TcSMUG S-derived Constructs—The FLAG-tagged version of a *TcSMUG S* full-length gene (GenBank™ Accession Number JN051960) from the SC43 cl92 stock has been described (30). This was cloned into the trypanosomatid expression vector *pTREX omni* to generate the *TcSMUG* construct. *pTREX omni* vector was generated by insertion of a XbaI-XhoI cassette bearing multiple cloning sites and a FLAG tag followed by GFP from *pDIY-eG* vector (GenBank™ Accession Number JN596089) into the *pTREXL-Neo* vector (GenBank™ Accession Number JN596094 (33).[6] *TcSMUG*Δ*GPI* and *TcSMUG*ΔΔ constructs were generated by PCR using the *TcSMUG* clone as template and oligonucleotides $TcSMUG_{fw}SP_{xba}$ and $TcSMUG_{fw}$-Thr_{xba}, respectively. In both reactions, the oligonucleotide $TcSMUG_{rev}Thr_{hind}$, which anneals to the FLAG tag in the *TcSMUG* clone (30) was used. Amplicons were treated with XbaI/HindIII, and ligated into *pTREX omni* vector previously digested with the same enzymes, thus lacking the GFP. *TcSMUG*Δ*SP* was generated by PCR using the *TcSMUG* clone as template and oligonucleotides $TcSMUG_{fw}Thr_{xba}$ and

[5] G. E. Cánepa, A. C. Mesías, H. Yu, X. Chen, and C. A. Buscaglia, unpublished results.

[6] L. A. Bouvier, M. M. Cámara, G. E. Cánepa, M. M. Miranda, and C. A. Pereira, submitted manuscript.

$TcSMUG_{rev}GPI_{spe}$. This amplicon was treated with XbaI/SpeI and ligated into *pTREX omni* vector previously digested with the same enzymes (also lacking the GFP). Sequence and features of every oligonucleotide used in this work are provided in supplemental Table S1.

TcSMUG S-derived Constructs Fused to GFP—TcSMUGΔGPI::GFP and *TcSMUGΔΔ::GFP* constructs were generated as their GFP-minus counterparts but using the reverse oligonucleotide $TcSMUG_{rev}Thr_{eco}$, which also anneals to the FLAG tag in the *TcSMUG* clone. Amplicons were XbaI/EcoRI digested, and ligated into *pTREX omni*, thus ensuing translational fusion to GFP. The *TcSMUGΔGPI::GFPA66* construct was generated by PCR using *TcSMUG* clone as template and oligonucleotides $TcSMUG_{fw}SP_{xba}$ and $TcSMUG_{rev}ThrN66_{cla}$. The amplicon was digested with XbaI/ClaI and ligated into *pTREX omni*. The *TcSMUG* GPI signal was amplified by PCR using the same template and oligonucleotides $TcSMUG_{fw}GPI_{hind}$ and $TcSMUG_{rev}GPI_{spe}$. This amplicon was digested with HindIII/SpeI and cloned into the likewise digested *TcSMUGΔGPI* and *TcSMUGΔΔ* clones to generate the *TcSMUG::GFP* and *TcSMUGΔSP::GFP* constructs, respectively.

TcMUC II-derived Constructs Fused to GFP—pTREX omni vector was also used to express variants of *RA-1* (GenBank™ Accession Number U32448), a *TcMUC II* gene from the RA parasite stock (34). *TcMUCΔGPI::GFP* and *TcMUCΔΔ::GFP* constructs were generated by PCR using the *RA-1* gene as template and the oligonucleotides $RA\text{-}1_{fw}SP_{xba}$ and $RA\text{-}1_{fw}Thr_{xba}$, respectively. In both cases, $RA\text{-}1_{rev}Thr_{cla}$ was used as reverse oligonucleotide. An intermediate construct spanning solely the *TcMUC* GPI signal was generated by PCR using the oligonucleotides $RA\text{-}1_{fw}GPI_{xba}$ and $RA\text{-}1_{rev}GPI_{xho}$, digested with XbaI/XhoI, and cloned into *pTREX omni* previously digested with SpeI/Xho. *TcMUCΔGPI::GFP* and *TcMUCΔΔGPI::GFP* clones were digested with XbaI/ClaI and the excised fragments ligated into the above mentioned clone to generate the *TcMUC::GFP* and *TcMUCΔSP::GFP* constructs, respectively. Cloning procedures were carried out in TOP10F bacteria (Invitrogen) and every construct was fully sequenced at our own facility.

Parasite Transfection—Epimastigotes (1.5×10^8) in exponential growth phase were transformed with 25 μg of purified DNA by electroporation and selected in BHT added with 20% FBS and 200 μg/ml G418 (Invitrogen). Transfected parasites were used as populations after at least 45 days of selection (30).

Nonidet P40-based Subcellular Fractionation—Parasites were washed with 0.25 M sucrose, 5 mM KCl, and kept frozen for 48 h, after which cells were thawed at 4 °C and resuspended in 50 mM Tris-HCl, pH 7.6, 0.15 M NaCl, 1 mM E-64 (Sigma). Following centrifugation for 10 min at 15,000 × *g*, the supernatant (cytosolic fraction) was removed and the pellet was resuspended in the same buffer supplemented with 1% Nonidet P40 (Nonidet P-40). The suspension was centrifuged as above and the supernatant (microsomal fraction) was collected (35). Aliquots were fractionated in 10–15% SDS-PAGE, transferred to PVDF membranes (GE Healthcare), and analyzed by Western blot using mAb anti-FLAG (clone M2, Sigma) at 1:5,000 dilution followed by HRP-conjugated secondary antibodies (Sigma) and chemiluminescence substrate (Pierce). For comparison purposes, samples were also probed by Western blot with antisera to RE markers *Tb*BiP (36) or *Tc*Calreticulin (35) (both at 1:3,000 dilution), or to cytosolic marker *Tc*PAbP (32) (1:1,000 dilution).

Secretion and Immunoprecipitation Assays—Parasites were washed and incubated at 28 °C for 3 h in serum-free BHT. Parasite suspension was centrifuged for 5 min at 3,500 × *g* and the final supernatant was filtered and used as conditioned medium (CM). Aliquots from the parasite pellet (P) and CM fractions were analyzed by Western blot using mAb 10D8 (23) (1:1,000 dilution). For immunoprecipitation, P and CM fractions were resuspended in ice-cold buffer (150 mM NaCl, 50 mM Tris.HCl, pH 7.6, 1 mM EDTA, 0.1% Nonidet P-40, 1% Triton X-100, 100 μM TLCK, 1 mM PMSF), and fractionated into 25 μl of mAb anti-FLAG-Sepharose (Sigma) as described (30). Bound fractions were analyzed by Western blot using rabbit antibodies to FLAG (1:3,000 dilution, Sigma) or mAb 10D8. When indicated, samples were processed for in-gel Western blot using rabbit anti-FLAG antibodies (1:2,000, Sigma) followed by rabbit IRDye 800CW antibodies (1:3,000, Li-Cor Biosciences) and labeled gels analyzed in an Odissey Infrared Imaging System (Li-Cor Biosciences) following manufacturer's specifications.

Concanavalin A-Sepharose Fractionation—Parasite pellets were resuspended at 1×10^7/ml in ConA buffer (50 mM Tris-HCl, pH 7.4, 150 mM NaCl, 1% Nonidet P-40, 0.1% Na deoxycholate, 1 mM PMSF, 50 μM TLCK, 1 mM DTT) and fractionated on 200 μl of concanavalin A-Sepharose (GE Healthcare). After washes, elution was carried out with 300 μl of ConA buffer added with 0.5 M α-methylmannoside (Sigma) (30). Bound and unbound fractions were analyzed by Western blot.

Purification of GPI-anchored Proteins—Pellets containing 1.5×10^8 parasites were homogenized in 2 ml of GPI buffer (10 mM Tris-HCl, pH 7.4, 150 mM NaCl, 2% Triton X-114 (TX-114), 1 mM PMSF and a protease inhibitor mixture (Sigma)) on ice for 1 h and the homogenate processed as described (37). Briefly, the homogenate was centrifuged at 8,800 × *g* for 10 min at 0 °C, and the supernatant (S1) was stored at −20 °C for 24 h. The pellet (P1) was washed with 1 ml of buffer A (10 mM Tris-HCl, pH 7.4, 150 mM NaCl, 0.06% TX-114, 1 mM PMSF), sonicated, and resuspended in denaturing loading buffer containing 6 M urea. S1 was thawed and submitted to phase separation at 37 °C for 10 min followed by centrifugation at 3,000 × *g* for 3 min at room temperature. The upper phase (S2) was collected and the detergent-rich phase re-extracted with 1 ml of buffer A. The upper phase (S3) was collected, and the detergent-rich phase was extracted with 1 ml of buffer A, homogenized, incubated for 30 min at 0 °C, and centrifuged at 18,000 × *g* for 10 min at 0 °C. The supernatant was submitted to a new phase separation after which the lower phase highly enriched in GPI-AMs was taken as GPI fraction. Equivalent aliquots of each fraction were precipitated in cold acetone, resuspended in denaturing loading buffer, and analyzed by Western blot.

Epi-Fluorescence Microscopy—Parasites were washed in PBS, fixed in PBS 4% *p*-formaldehyde (PBS-PAF) for 10 min and processed for fluorescence microscopy or indirect immunofluorescence (IIF) assays (22, 38). The indicated antisera and mAb anti-FLAG were used at 1:500 dilution. Analysis was performed in a Nikon Eclipse E600 microscope coupled to a SPOT RT

color camera (Diagnostic Instruments, Inc.), and images were processed using ImageJ.

Flow Cytometry—Live parasites (1×10^6/ml) were incubated in an ice-water bath for 20 min in PBS supplemented with 3% FBS followed by 20 min of incubation with mAb anti-FLAG at 1:500 dilution. Epimastigotes were washed with PBS and labeled with Alexa Fluor 488-conjugated secondary antibodies (Invitrogen). After 20 min, cells where washed, resuspended in 300 μl of PBS-PAF, and analyzed using fluorescence-activated cell sorting CyFLOW Partec and FloMax software.

Sialic Acid Labeling—Epimastigote forms extensively washed in cold PBS were labeled for 30 min at room temperature in the presence of 30 ng of recombinant *T. cruzi* TS (39), 10 mM 2-deoxyglucose (Sigma) and 1 mM of the azido-sialyllactose analog Neu5Azα2–3LacβOMe as sialyl residue donor (40). Reaction was heated at 65 °C to inactivate TS and non-permeabilized parasites labeled by the Staudinger method with 250 μM Phosphino-biotin (Sigma) for 16 h at room temperature. As a result, labeled glycoconjugates displayed a biotin group covalently attached to the Neu5Az residue. The exquisite chemical selectivity of the overall system has been recently demonstrated (30). Western blot membranes were probed with avidin-HRP (R&D, 1:200 dilution) followed by chemilluminescent substrate. Alternatively, labeled epimastigotes were centrifuged and both, parasite lysates and the CM were independently fractionated onto 25 μl of StreptAvidin-agarose (Sigma) as described (30). Bound and unbound fractions were analyzed by Western blot.

RESULTS

Expression of TcSMUG Deletion Mutants in T. cruzi Epimastigotes—As a first step toward the study of mucin trafficking and processing in *T. cruzi*, we generated a panel of FLAG-tagged variants on the backbone of a *TcSMUG S* representative gene (Fig. 1*A*). The deduced product of this construct (henceforth termed *TcSMUG*) contains a 24 aa-long SP followed by a 61-aa long central domain, which includes a single *N*-linked glycosylation site and a FLAG epitope, and a 29-aa long GPI attachment signal (30). Importantly, recombinant TcSMUG was shown to be displayed on the surface of transfected epimastigotes as a GPI-anchored, mucin-type glycoconjugate, indistinguishable from endogenous Gp35/50 mucins (30). *TcSMUG* and all of its derivatives were transfected into epimastigotes of the Adriana stock, which was typed within the TcI evolutionary lineage (30). None of the constructs led to a noticeable growth phenotype upon transfection in epimastigotes (not shown). After 45 days of selection, transfected parasites were analyzed for the expression of FLAG-containing products by non-permeabilizing flow cytometry, upon reaction of live epimastigotes with mAb anti-FLAG (Fig. 1*B*). Control parasites were either non-transfected, which yielded no signal when probed with the anti-FLAG mAb (not shown), or transfected with *TcSMUG*, which yielded typical peripheral labeling over the entire parasite on IIF assays. The fact that only a fraction (~40%) of gated *TcSMUG*-transfected epimastigotes displayed high fluorescence intensity is compatible with them being used as whole populations, thus bearing a mixture of high- and low-expressing parasites (Fig. 1*B*).

Simultaneous deletion of the SP and the GPI-anchoring signal led to plasma membrane exclusion of TcSMUGΔΔ (Fig. 1*B*). TcSMUGΔΔ seemed to localize to the cytoplasm of transfected parasites, and IIF co-localization assays with *Tc*PAbP1, a polyadenylated mRNA-binding protein with exclusive cytoplasmic localization (32), indeed showed substantial overlapping of the signals except for the parasite nuclei, from where *Tc*PAbP was largely excluded (Fig. 1*C*).

IIF studies showed the intracellular accumulation of FLAG-reactive granules, *i.e.* round structures variable in size and up to ~0.3 μm across in diameter, in *TcSMUGΔSP*-transfected parasites (Fig. 1*C*). The molecular basis underlying formation and composition of these granules was not further explored, although a possible interpretation would be that, in common with other amphipathic molecules (41), TcSMUGΔSP forms micellar structures with the uncleaved, highly hydrophobic GPI-anchoring signal at the very core. Subcellular fractionation assays showed that TcSMUGΔSP localized exclusively to the cytoplasm (Fig. 1*D*). This finding indicated that, in the absence of the SP, the GPI attachment signal could not redirect the construct to the secretory pathway, as verified in other systems (42). To further address this issue, we purified total GPI-AMs from *TcSMUGΔSP*-transfected parasites taking advantage of their preferential fractionation in TX-114 (37), and aliquots corresponding to the different fractions were analyzed by Western blot. FLAG reactivity was restricted to the pellet (P1), containing parasite nuclei and cytoskeletal structures, and aqueous fractions (S1, S2), composed largely of cytoplasmic molecules (Fig. 1*E*). An additional ~27 kDa band was observed in the S2 fraction, but whether this corresponded to TcSMUGΔSP aggregates or post-translationally modified molecules was not further investigated. Importantly, TcSMUGΔSP was completely excluded from the final GPI-AMs-enriched fraction (termed GPI), thus ruling out processing of the GPI-anchoring signal, and hence ER import, of this product.

We next analyzed the TcSMUGΔGPI product bearing deletion immediately downstream of the GPI acceptor residue. IIF assays showed a punctate pattern throughout the cell body (Fig. 1*C*). When parasites were co-stained with antisera raised against the *T. brucei* chaperone BiP or *Tc*Calreticulin (both well-established ER markers), the pattern of co-localization suggested that TcSMUGΔGPI was (at least partially) located in this compartment (Fig. 1*C* and not shown). Subcellular fractionation assays further supported microsomal accumulation of TcSMUGΔGPI (Fig. 1*D*). Co-localization studies with markers from additional compartments of the secretory pathway showed that neither the Golgi stacks marker GRASP (43) nor did the reservosome marker cruzipain (35) display substantial overlap with TcSMUGΔGPI (Fig. 1*F*).

Taken together, these results indicate that (i) the TcSMUG SP is functional and essential for targeting these products to the ER, and (ii) lack of a C-terminal GPI-anchor determines retention of TcSMUG products within the secretory pathway, most likely in the ER.

Trafficking Signals Are Functionally Conserved in T. cruzi Mucin-type Products—Even though the TcSMUGΔGPI products could not be detected on the parasite surface (Fig. 1*C*), the fact that they gained access to the secretory pathway suggested

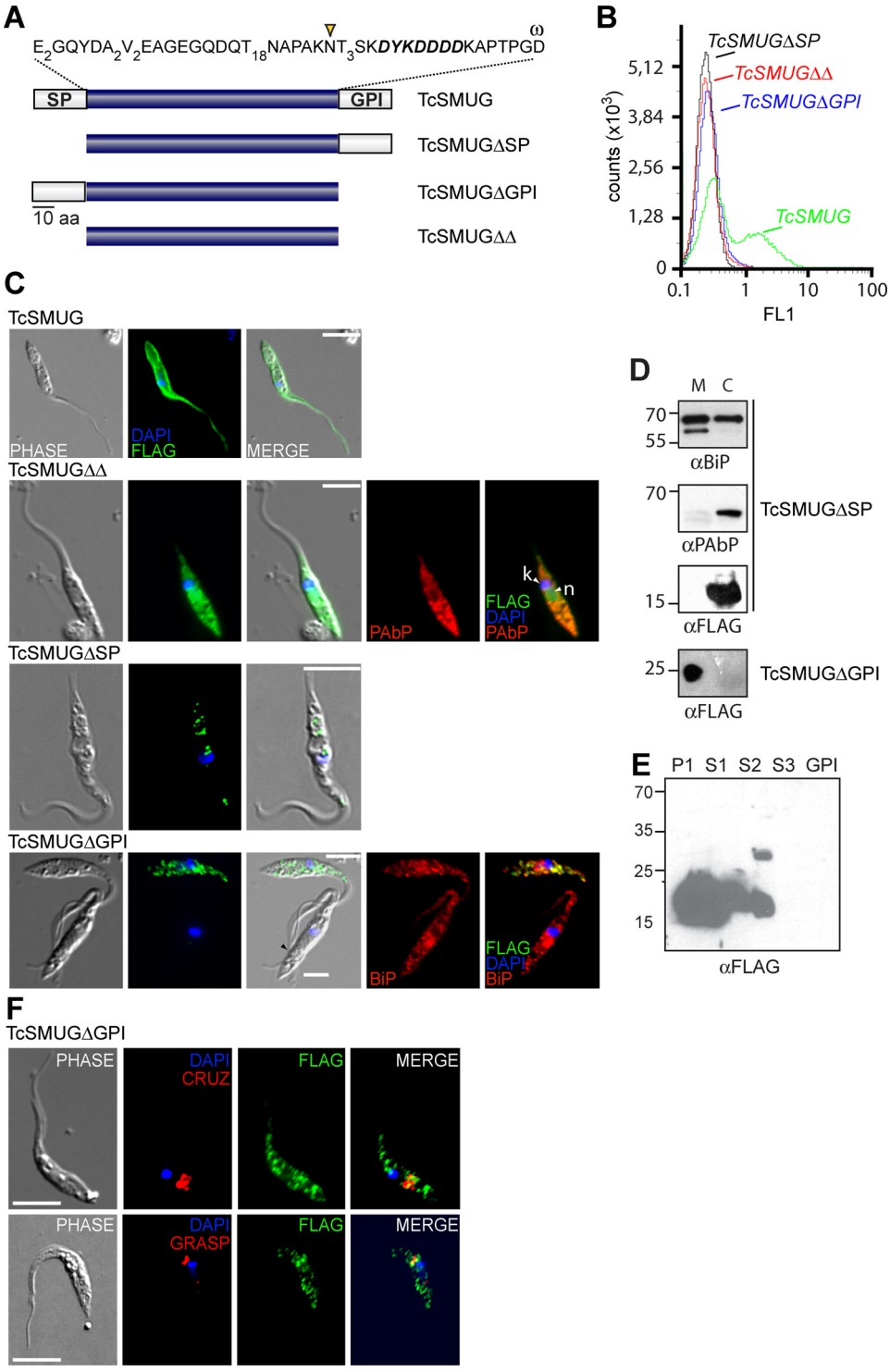

FIGURE 1. **Expression and localization of TcSMUG variants in *T. cruzi* epimastigotes.** *A*, schematic in-scale illustration of TcSMUG reporters. The sequence of the central domain (*blue*), which includes a single *N*-linked glycosylation site (residue Asn-66, *arrowhead*), the FLAG epitope (*bold italics*), and the glycolipid acceptor residue (Asp-78, ω) is indicated. *SP*, Signal peptide; *GPI*, GPI-anchoring signal. *B*, live epimastigotes transfected with the indicated construct were reacted with mAb anti-FLAG and evaluated by flow cytometry. Representative results of at least three experiments are shown. Note that only a fraction (40.37%) of the *TcSMUG*-transfected population shows above-the-threshold fluorescence, denoting detectable expression levels. *C*, epimastigotes expressing the indicated fusion protein were permeabilized and analyzed by indirect immunofluorescence (*IIF*) assays using mAb anti-FLAG (*green*). DAPI signals are shown in *blue*. Bars, 10 μm. TcSMUGΔΔ- and TcSMUGΔGPI-transfected parasites were co-labeled with rabbit antiserum against *Tc*PAbP (cytoplasmic marker, *red*) and *Tb*BiP (ER marker, *red*), respectively. Kinetoplast (*k*) and nucleus (*n*) are indicated with *white arrowheads*. Epimastigotes showing undetectable expression levels are indicated with *black arrowheads*. *D*, epimastigotes expressing the indicated fusion protein were fractionated following a Nonidet P-40-based method and samples from the cytoplasm (*C*) and microsomes (*M*) were probed with the indicated antibody. Cellular distribution of ER marker BiP and cytoplasmic marker PAbP is shown for comparison purposes. *E*, epimastigotes transfected with the TcSMUGΔSP construct were fractionated with Triton X-114, and aliquots of each fraction (see "Experimental Procedures") were probed with mAb anti-FLAG. Molecular markers (in kDa) are indicated. *F*, TcSMUGΔGPI labeled with mAb anti-FLAG (*green signals*) shows neither substantial co-localization with *Tc*Cruzipain (*red signals*, upper panels), which labels the reservosome, nor with *Tc*GRASP (*red signals*, lower panels), which labels the Golgi stacks.

that, at least a fraction, may became secreted. To evaluate this possibility, we carried out Western blot analyses on the conditioned medium (CM) of *TcSMUGΔGPI*-transfected parasites, which rendered consistently negative results (see below). It is worth mentioning, however, that several antibodies directed against GPI-AMs reacted very poorly, if at all, with the cognate protein upon cleavage of the GPI-anchor through phosphoinositol-specific phospholipase C treatment (44). The same phenomenon was observed for different *T. cruzi* mucin-type species (24, 30, 45, 46). Schenkman *et al.* put forward the idea that the extremely hydrophilic character of *T. cruzi* mucins impaired their binding to membrane supports, *i.e.* Nitrocellulose or PVDF, once the lipid moiety was removed (45). In such a case, and if undergoing mucin-type processing along its further trafficking through the secretory pathway, it would be expected that secreted TcSMUGΔGPI, lacking GPI anchorage, also display restricted binding to membrane supports. To overcome this limitation, we generated a series of protein reporters, including a version of the *TcSMUGΔGPI* construct, bearing GFP fusion downstream of the FLAG epitope (supplemental Fig. S1). In addition of aiding in the tracing of transgenic molecules, we hypothesized that GFP would provide a bulky amphipathic motif to the overall product, thus enabling its detection by Western blot. To expand our analyses, we generated a similar series of reporters based on a representative member of the *TcMUC II* group (supplemental Fig. S1), which provides peptide scaffolds for bloodstream trypomastigote mucins (22). A full-length version of this particular *TcMUC II* construct, though lacking GFP, was shown to be displayed on the surface of transfected Adriana epimastigotes as a GPI-anchored, mucin-type species.[5]

Epimastigotes transfected with each GFP-bearing construct were analyzed for the expression of recombinant products as above. No viable overexpressing parasites were recovered after several independent transfection attempts using the full-length reporters (TcSMUG::GFP and TcMUC::GFP). The reasons for this are not clear, although anecdotal and published data (47) also indicate negative growth phenotypes upon expression of non-trypanosomal GPI-anchored reporters (including GFP) in trypanosomes. As for the rest of the products (ΔSP::GFP, ΔGPI::GFP, and ΔΔ::GFP variants), they were trafficked and processed largely as their corresponding GFP-minus counterparts.

Briefly, both ΔΔ::GFP variants showed diffuse localization throughout the entire cytoplasm (Fig. 2, *A* and *B*). At variance with the TcSMUGΔΔ reporter, and likely due to their larger size (M_r ~45 and ~52 kDa for TcSMUGΔΔ::GFP and TcMUCΔΔ::GFP, respectively (Fig. 2*B*)), passive diffusion of these molecules through the nuclear pore was impaired (48). On the other hand, we noticed the formation of GFP-bearing "granules" in TcSMUGΔSP::GFP-expressing parasites (Fig. 2*C*), much alike to what has been observed in TcSMUGΔSP-expressing ones. Again, TcSMUGΔSP::GFP was excluded from the final GPI-AMs-enriched fraction, consistent with its cytoplasmic localization (Fig. 2, *D* and *E*). Oddly, and despite RT-PCR analyses indicating mRNA expression, no specific signal was detected by fluorescence microscopy or Western blot assays in parasites transfected with the *TcMUCΔSP::GFP* construct (not shown). Whether this was due to protein toxicity, post-transcriptional regulation mechanisms and/or other alternative was beyond the aims of this study and not further pursued. Most importantly, and consistent with results described for TcSMUGΔGPI, both ΔGPI::GFP products showed several features supporting their ER accumulation (Fig. 2, *F* and *G*). In Nonidet P-40-based experiments, they largely partitioned to the microsomal fraction, and fluorescence microscopy assays indicated accumulation of these products in discrete patches concentrated in the perinuclear area, typical of ER-resident molecules (49). Indeed, co-localization assays with BiP showed almost complete overlapping of the signals.

In summary, these results provide strong support to the main conclusions highlighted in the previous section. Together with previous findings in TcMUC molecules transgenically expressed in epimastigote forms (24, 50),[3] they also indicate a high degree of correspondence, which is consistent with the overall structural similarity of their encoded signals (supplemental Fig. S1), in the trafficking of TcSMUG and TcMUC products.

TcSMUGΔGPI::GFP Products Are Secreted as Fully Processed Mucins—Going back to the original issue, that is, the putative secretion of GPI-minus products, parasites were incubated in serum-free medium for 3 h and both the parasite pellets and the CM fractions were analyzed by Western blot. FLAG-reactive signals were indeed detected in the CM of *TcSMUGΔGPI::GFP*- and *TcMUCΔGPI::GFP*-transfected parasites but not in the CM of *TcSMUGΔGPI*-transfected ones (Fig. 3*A*). When we carried out in-gel Western blot, however, a ~25 kDa, FLAG-reactive band was detected in the CM of *TcSMUGΔGPI*-transfected parasites (Fig. 3*B*), indicating that this product is secreted but impaired in its binding to membrane supports. These findings support GFP-translational fusion as an appropriate strategy to overcome Western blot detection limitations of anchorless mucins. FLAG-reactive signals were neither detected in the CM of TcSMUGΔΔ::GFP-expressing parasites (Fig. 3*A*), thus ruling out significant parasite lysis during the assay, nor in the CM of epimastigotes transfected with *pTREX omni* vector. The latter expressed high amounts of FLAG-tagged GFP in the cytoplasm, thus arguing against a possible "spill-over" effect in our system.

Besides secretion, one interesting finding was that, for TcSMUGΔGPI and for both ΔGPI::GFP reporters, the apparent molecular mass of secreted products was larger than that of the intracellularly accumulated counterparts (compare *CM* and *P lanes* in Fig. 3). This shift suggested that anchorless products underwent further processing, and particularly *O*-glycosylation, in post-ER compartments before being secreted into the medium. To evaluate this possibility, we probed parasite extracts and CM fractions with a monoclonal antibody (mAb 10D8) directed toward Gal*f*-based epitopes that decorate *O*-type glycans in mature, surface-associated Gp35/50 mucins from TcI parasites (23). A distinctive ~55–60 kDa signal, very reminiscent of the secreted TcSMUGΔGPI::GFP product itself (Fig. 3), was detected in the CM of *TcSMUGΔGPI::GFP*-transfected parasites (Fig. 4*A*). This signal was also observed, although to a much lesser extent, in the parasite fraction, likely due to cross-contamination with the CM fraction (see below). In contrast, only the signal corresponding to

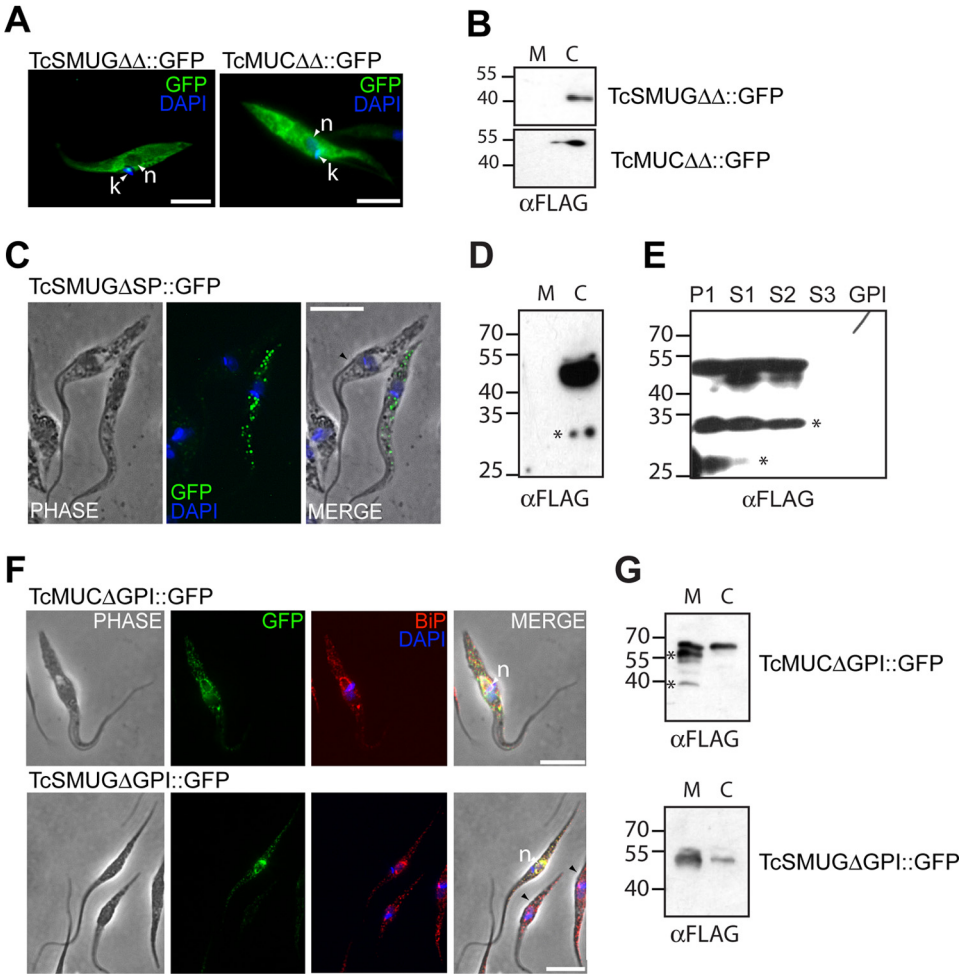

FIGURE 2. **Expression and localization of TcSMUG::GFP and TcMUC::GFP variants in *T. cruzi* epimastigotes.** *A*, *C*, *F*, *T. cruzi* epimastigotes expressing the indicated GFP fusion protein were analyzed by immunofluorescence microscopy (*green signals*). DAPI signals are shown in *blue*. Bars, 10 μm. Kinetoplast (*k*) and nucleus (*n*) are indicated with *white arrowheads*. When indicated, parasites were permeabilized and labeled by indirect immunofluorescence (*IIF*) assays using an antiserum to *Tb*BiP (ER marker, *red*). Epimastigotes showing undetectable expression levels are indicated with *black arrowheads*. *B*, *D*, *G*, epimastigotes transfected with the indicated construct (in *panel D*, transfected with *TcSMUGΔSP-GFP*) were fractionated following a Nonidet P-40-based method and samples from the cytoplasm (*C*) and microsomes (*M*) were probed with mAb anti-FLAG. *E*, epimastigotes transfected with the *TcSMUGΔSP-GFP* construct were fractionated with Triton X-114 and aliquots of each fraction (see "Experimental Procedures") were probed with mAb anti-FLAG. *Asterisks* denote degradation products. Molecular markers (in kDa) are indicated.

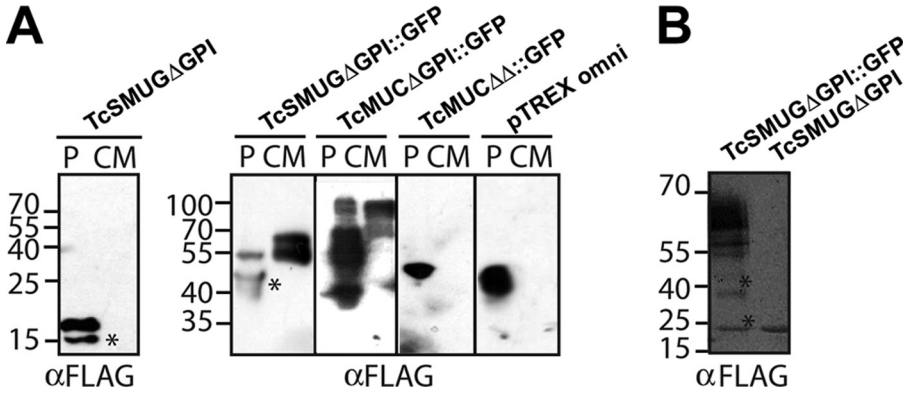

FIGURE 3. **Secretion of TcSMUGΔGPI::GFP and TcMUCΔGPI::GFP transgenic products.** *A*, epimastigotes transfected with the indicated construct were incubated in serum-free medium and the conditioned medium (*CM*) and parasite pellet (*P*) fractions were probed by Western blot with mAb anti-FLAG. *B*, epimastigotes transfected with the indicated construct were incubated in serum-free medium and the CM fractions were probed by in-gel Western blot with mAb anti-FLAG. *Asterisks* denote degradation products. Molecular markers (in kDa) are indicated.

endogenous Gp35/50 mucins was detected in TcSMUGΔGPI- and TcMUCΔGPI::GFP-expressing parasites upon labeling with mAb 10D8.

To address the nature of the additional signal observed in TcSMUGΔGPI::GFP-expressing parasites, parasite lysates and CM were independently fractionated using FLAG affinity chro-

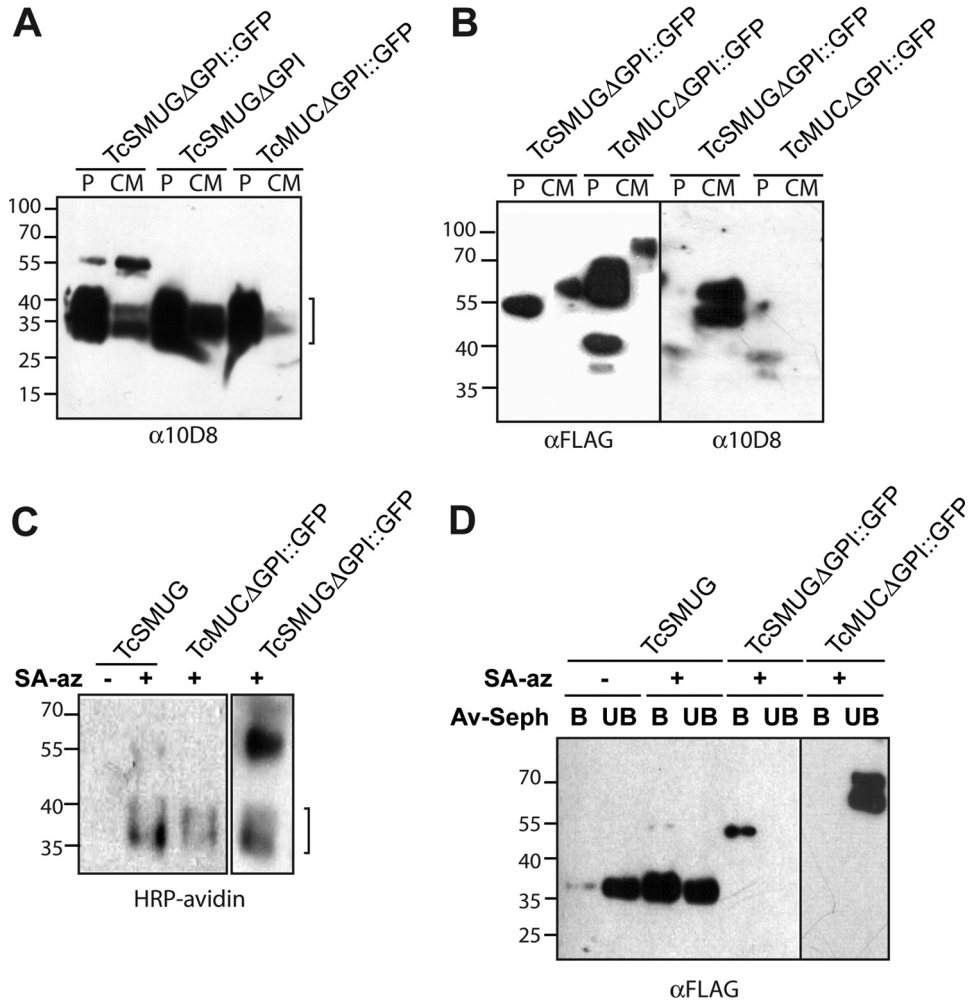

FIGURE 4. **TcSMUGΔGPI::GFP is secreted as a fully processed mucin.** *A*, epimastigotes transfected with the indicated construct were incubated in serum-free medium and the conditioned medium (*CM*) and parasite pellet (*P*) fractions were probed with mAb 10D8. Signals provided by endogenous Gp35/50 mucins are indicated by a *bracket*. *B*, CM and P fractions from the indicated parasites were fractionated onto mAb anti-FLAG-Sepharose and retained fractions probed with rabbit antibodies to FLAG (*left panel*) or mAb 10D8 (*right panel*). *C*, suspensions of parasites expressing the indicated protein were labeled (+) or not (−) with Neu5Azα2–3LacβOMe (SA-az) followed by reaction of the azido group with a phosphine-tagged biotin, lysed, and probed with HRP-avidin by Western blot. Signals provided by endogenous Gp35/50 mucins are indicated by a *bracket*. *D*, lysates from the indicated parasites were labeled (+) or not (−) as in *C*, fractionated onto StreptAvidin-agarose and both flow-through (*UB*) and retained (*B*) fractions were probed with mAb anti-FLAG. Molecular markers (in kDa) are indicated.

matography and analyzed by Western blot. The secreted TcSMUGΔGPI::GFP product, but not the ER-retained one, beared mAb 10D8-reactive epitopes (Fig. 4*B*). In the case of TcMUCΔGPI::GFP, although both the intracellular and secreted forms were efficiently immunoprecipitated, neither one of them reacted with mAb 10D8.

Another diagnostic feature of mature TcSMUG products is the presence of terminal βGal*p* residues, which could be extracellularly decorated with SA residues through the action of TS molecules (21). To test whether secreted TcSMUGΔGPI::GFP may also function as SA acceptor, we carried out sialylation assays over parasites incubated in the presence of exogenously added *T. cruzi* TS, as epimastigote forms express low amounts of this enzyme, and Neu5Azα2–3LacβOMe as sialyl residue donor (40). The azido group of Neu5Az incorporated in parasite-associated or secreted glycoproteins is then reacted with a phosphine-tagged biotin thus leading to the formation of a SA-biotin group, which can be detected by Western blot. Control experiments carried out in the absence of Neu5Azα2–3LacβOMe rendered negative results, ensuring the specificity of the overall system. Initial sialylation experiments in *TcSMUG*-transfected parasites showed the incorporation of SA residues in a smear corresponding to the endogenously expressed Gp35/50 mucins (Fig. 4*C*). The ectopically expressed *TcSMUG* construct was also labeled with SA but did not render an additional band since, as expected, it co-migrated with endogenous Gp35/50 mucins (30). Note that the proportion of this ~35 kDa product retained by avidin chromatography was significantly increased upon Neu5Azα2–3LacβOMe labeling (Fig. 4*D*). Importantly, the secreted TcSMUGΔGPI::GFP product, but not the TcMUCΔGPI::GFP one, functioned as an effective acceptor of SA residues in the TS-catalyzed reaction. Together with mAb 10D8 results, these findings indicate (i) that GPI-minus reporters that achieve to exit the putative retention mechanism undergo *O*-glycosylation in post-ER compartments and are ultimately secreted as mature mucin-type glycopro-

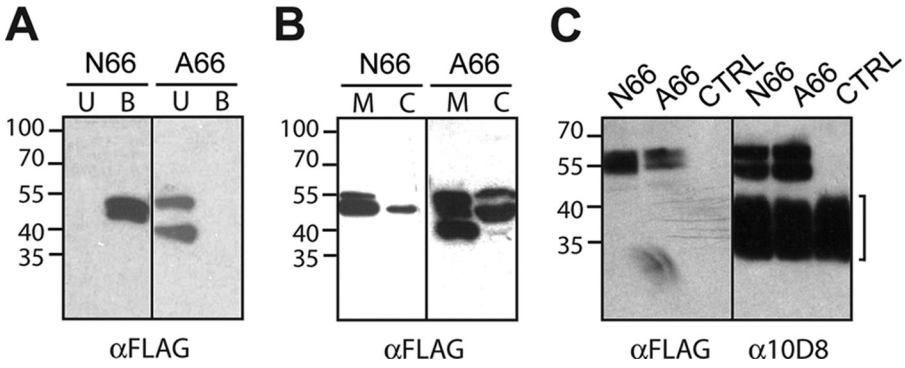

FIGURE 5. ***O*-Glycan addition and secretion of TcSMUGΔGPI::GFP is independent of its *N*-glycosylation motif.** *A*, lysates from epimastigotes expressing the TcSMUGΔGPI::GFP reporter (N66) or its mutant version in which Asn-66 was changed to Ala (A66) were fractionated onto concanavalinA-Sepharose and both flow-through (*UB*) and retained (*B*) fractions were probed with mAb anti-FLAG. *B*, epimastigotes expressing the indicated protein were fractionated following a Nonidet P-40-based method and samples from the cytoplasm (*C*) and microsomes (*M*) were probed with mAb anti-FLAG. *C*, epimastigotes transfected with the indicated construct or nontransfected (*CTRL*) were incubated in serum-free medium and the conditioned media were probed either with mAb anti-FLAG or mAb 10D8. In the latter case, signals provided by endogenous Gp35/50 mucins are detected (*bracket*). *Asterisks* denote degradation products. Molecular markers (in kDa) are indicated.

teins, and (ii) that TcSMUG and TcMUC reporters are differentially recognized and processed by the epimastigote *O*-glycosylation machinery.

N-Glycan Addition Is Dispensable for Mucin-type Processing and Secretion—To evaluate a putative role of *N*-glycans in the trafficking/maturation of *T. cruzi* mucins, we generated a TcSMUGΔGPI::GFP site-specific mutant in which the Asn-66 residue of its unique *N*-glycosylation site (Fig. 1*A*) was changed to Ala. This construct, termed *TcSMUGΔGPI::GFPA66* or *A66*, was transfected and analyzed essentially as before. To check for the effective disruption of the *N*-glycosylation signal, parasite lysates were fractionated by concanavalin A chromatography. The A66 variant was recovered in the unbound fraction whereas the parental N66 molecule only eluted from the resin upon addition of the α-methylmannoside (Fig. 5*A*). Despite this, IIF and subcellular fractionation assays indicated that both A66 and N66 products showed indistinguishable localization (Fig. 5*B* and supplemental Fig. S2). Moreover, both molecules underwent similar maturation process, as judged by the acquisition of 10D8-reactive epitopes and similar increase in molecular size before being secreted roughly in the same amounts to the extracellular medium (Fig. 5*C*). Together, these findings indicate that *N*-glycan addition/maturation is dispensable for TcSMUG processing and secretion.

DISCUSSION

With as much as 4×10^6 molecules per parasite, mucins constitute one of the major GPI-AMs in every developmental form of *T. cruzi* (16). Despite the sheer numbers and relevant roles for parasite growth and infectivity, methodological issues have so far curtailed detailed studies on these molecules. In this work, we aimed to dissect the contribution of distinct post-translational modifications on their trafficking, maturation, and secretion using the fidelity of a homologous expression system. Although we analyzed a single variant for each group (*TcSMUG* or *TcMUC*), the high degree of conservation of trafficking signals among members of either gene family (16), and even between them, allows in principle to generalize our results for every mucin in *T. cruzi*.

The major conclusion that can be drawn out from these studies is that the absence of GPI anchor leads to the accumulation of immature apo-mucins in the early secretory pathway, most likely in the ER, of insect-dwelling epimastigote forms. Notably, a few GPI-minus reporters eventually escape this retention mechanism and become secreted as mature mucin-type molecules. At variance with TcSMUG reporters, and although they showed a ~20 kDa shift as compared with their ER-retained counterparts, TcMUC reporters do not acquire typical Gp35/50 mucin glycomarkers such as mAb 10D8-reactive epitopes or terminal βGal*p* residues in the proper configuration as to become SA acceptors. Although mass spectrometric analyses of TcMUC transgenic products will be required to address the structure of attached oligosaccharides, GPI-AMs undergoing extensive glycosylation at Ser/Thr residues but lacking terminal Gal residues have been described in the epimastigote surface (51).

Differential processing of TcMUC and TcSMUG reporters reveals the presence of mucin-specific sequence/structure determinants, which can be told apart by the *O*-glycosylation machinery in *T. cruzi* epimastigotes. This is consistent with our previous results, in which we showed that epimastigotes with the same genetic background were able to discriminate, and process accordingly, even between highly related TcSMUG S and L transgenic products (30). Interestingly, epimastigote-expressed TcMUC reporters neither acquired glycomarkers typical of bloodstream trypomastigote mucins.[5] A plausible interpretation would be that some of the glycosyltransferases, carbohydrate epimerases, and/or glycosidases required to elaborate trypomastigote-restricted glycomarkers are not present in the epimastigote forms. Taking into account that attached carbohydrates drive most of functional aspects of *T. cruzi* mucins, such level of complexity and optimization of the *O*-glycosylation machinery could reflect another level for differential regulation of "protein expression" in an organism that appears to largely bypass regulation of transcription initiation.

The phenomenon of ER-accumulation is restricted to the GPI-minus reporters. Since the amount of endogenous

Gp35/50 mucins was not significantly affected in transfected parasites as compared with nontransfected controls (see Fig. 5*C*, *right panel*) it cannot be attributed to a global trafficking depression due to ER stress or saturation of transport mechanisms. As for the molecular basis underlying this observation, two alternative hypotheses can be envisaged. On one hand, it is possible that ΔGPI reporters, which are normally membrane bound, are unable to attain a stable conformation when expressed in soluble form and are thus retained in the ER by folding quality control systems (35). Experiments aimed at quantifying the association of GPI-minus reporters with BiP and/or other molecular chaperones may shed some light on this issue. In this line, however, it is worth noting that calreticulin, the main *N*-glycoprotein chaperone in *T. cruzi* (35), does not seem to play a significant role in apo-mucin maturation/trafficking, as revealed by the A66 mutant. Further evidence weigh against "quality control" as a mechanism for regulating export of ΔGPI reporters. Firstly, *T. cruzi* mucins, unlike mammalian ones (52), do not form intra- or inter-molecular disulfide bonds as part of their folding process. Neither them are predicted to adopt local or global complex three-dimensional conformations. Secondly, we did not find evidence supporting degradation of "misfolded" GPI-minus products either in reservosomes or in proteasomes following their retrotranslocation to the cytoplasm. Moreover, secreted TcSMUG GPI-minus products display several features diagnostic of mature mucin-type molecules, thus indicating that elimination of the GPI anchor does not impair their proper processing and maturation.

We rather favor a second hypothesis, which is supported by phylogenetic data and which poses that the GPI moiety itself constitutes a forward transport signal within the secretory pathway, by conferring some physical/chemical property, which improves the timely forward transport of attached apomucins. In concordance with recent models of vesicular transport in eukaryotes (8, 9, 12, 13), this hypothesis implies that the GPI anchor triggers cargo discrimination at ERES, which facilitates selective entry of GPI-AMs into budding, COPII coated secretory vesicles. The capacity of GPIs to act as sorting signals could rely either on their affinity for membrane lipid microdomains enriched with cholesterol and sphingolipids or, alternatively, on their binding to specific receptor(s) that mediate vesicle loading. In support of the latter aspect, a p24-based mechanism for selective GPI-anchored cargo loading into COPII vesicles has been recently unraveled in the highly related parasite *T. brucei* (13). Together with a remarkable degree of "streamlining" architecture in the early secretory pathway, this mechanism is likely to maximize efficiency of variant surface glycoprotein (VSG) transport to the *T. brucei* surface. Interestingly, studies with VSG reporters led to similar findings than those presented here. Briefly, deletion of the GPI signal was shown to significantly reduce the rate of VSG transport to the plasma membrane relative to GPI-anchored controls in fly-dwelling procyclic forms (36, 53, 54). GPI-minus VSG variants accumulated in the ER but they were nonetheless finally secreted in small amounts (53). At odds with our *T. cruzi* mucin system, however, point mutation(s) on the *N*-glycosylation sites reduced VSG expression up to 15-fold (47). GPI addition was also shown to positively affect trafficking of Gp63, one of the major GPI-AM in *Leishmania* promastigotes (55–57). Overall, and besides minor variations depending on the species, developmental stage and/or reporter molecules, trypanosomatids seem to have evolved a fine-tuned transport mechanism for improved secretion of their GPI-AMs to the point of over-reliance. As a result of the need to efficiently transport large amounts of mucins, and although further studies are required to address the underlying molecular basis, our results likely point to a similar phenomenon, in which GPI-anchors are recognized as positive forward transport signals, in *T. cruzi*.

From a functional standpoint, our findings open an even more interesting possibility that deserves to be explored. *T. cruzi* genomic data indicate that a significant proportion (~25%) of mucin-type genes, and particularly from the *TcMUC II* group, bear translation termination codons in their central domains (17, 58). Although mRNA expression for some of them has been demonstrated (58), these arbitrarily called "pseudogenes" were thought to be conserved merely as an additional pool of genetic variability for the generation of new mucin variants through recombination/gene conversion mechanisms (17). Interestingly, their predicted products present structural features (overall amino acid composition, extensive number of potentially *O*-glycosylation sites) as to be considered mucin-type products. So, translation of some of these "pseudogenes" is likely to generate molecules structurally related to the ΔGPI reporters analyzed here. ER-accumulation and/or constitutive secretion of anchorless mucin-type molecules could actively contribute in shaping the parasite/host interplay.

Acknowledgments—We thank Drs. L. Bouvier and C. Pereira (Instituto de Investigaciones Médicas Alfredo Lanari, Buenos Aires, Argentina) for providing us the pTREX omni vector, Dr. J. Mucci (IIB-INTECH) for purified TS, Dr. N. Yoshida (UNSP, Brazil) for kindly providing mAb 10D8, Dr. J. Bangs for the anti-TbBiP antiserum, Dr. A. Cassola (IIB-INTECH) for the anti-TcPAbP antiserum, Dr. C. He (National University of Singapore) for the anti-TbGRASP antiserum, Dr. C. Labriola (FIL, Buenos Aires, Argentina) for the anti-Tc-Calreticulin antiserum, and Drs. J. Ugalde (IIB-INTECH), Daiana Sapochnik and Omar Coso (FCEyN-UBA, Buenos Aires, Argentina) for reagents and assistance with the in-gel Western blots. We are also indebted to A. Chidichimo, L. Sferco, and B. Franke de Cazzulo for culturing parasites. Critical reading of the manuscript by Dr. J. Di Noia is appreciated.

REFERENCES

1. Ferguson, M. A. (1999) The structure, biosynthesis and functions of glycosylphosphatidylinositol anchors, and the contributions of trypanosome research. *J. Cell Sci.* **112,** 2799–2809
2. Maeda, Y., and Kinoshita, T. (2011) Structural remodeling, trafficking and functions of glycosylphosphatidylinositol-anchored proteins. *Prog Lipid Res* **50,** 411–424
3. Fraering, P., Imhof, I., Meyer, U., Strub, J. M., van Dorsselaer, A., Vionnet, C., and Conzelmann, A. (2001) The GPI transamidase complex of Saccharomyces cerevisiae contains Gaa1p, Gpi8p, and Gpi16p. *Mol. Biol. Cell* **12,** 3295–3306
4. Kawagoe, K., Kitamura, D., Okabe, M., Taniuchi, I., Ikawa, M., Watanabe, T., Kinoshita, T., and Takeda, J. (1996) Glycosylphosphatidylinositol-anchor-deficient mice: implications for clonal dominance of mutant cells in paroxysmal nocturnal hemoglobinuria. *Blood* **87,** 3600–3606
5. Munro, S. (2003) Lipid rafts: elusive or illusive? *Cell* **115,** 377–388

6. Medof, M. E., Nagarajan, S., and Tykocinski, M. L. (1996) Cell-surface engineering with GPI-anchored proteins. *Faseb J* **10,** 574–586
7. Schuck, S., and Simons, K. (2006) Controversy fuels trafficking of GPI-anchored proteins. *J. Cell Biol.* **172,** 963–965
8. Muñiz, M., Morsomme, P., and Riezman, H. (2001) Protein sorting upon exit from the endoplasmic reticulum. *Cell* **104,** 313–320
9. Hughes, H., and Stephens, D. J. (2008) Assembly, organization, and function of the COPII coat. *Histochem Cell Biol.* **129,** 129–151
10. Bonnon, C., Wendeler, M. W., Paccaud, J. P., and Hauri, H. P. (2010) Selective export of human GPI-anchored proteins from the endoplasmic reticulum. *J. Cell Sci.* **123,** 1705–1715
11. Strating, J. R., and Martens, G. J. (2009) The p24 family and selective transport processes at the ER-Golgi interface. *Biol. Cell* **101,** 495–509
12. Castillon, G. A., Aguilera-Romero, A., Manzano-Lopez, J., Epstein, S., Kajiwara, K., Funato, K., Watanabe, R., Riezman, H., and Muñiz, M. (2011) The yeast p24 complex regulates GPI-anchored protein transport and quality control by monitoring anchor remodeling. *Mol. Biol. Cell* **22,** 2924–2936
13. Sevova, E. S., and Bangs, J. D. (2009) Streamlined architecture and glycosylphosphatidylinositol-dependent trafficking in the early secretory pathway of African trypanosomes. *Mol. Biol. Cell* **20,** 4739–4750
14. Rivier, A. S., Castillon, G. A., Michon, L., Fukasawa, M., Romanova-Michaelides, M., Jaensch, N., Hanada, K., and Watanabe, R. (2011) Exit of GPI-anchored proteins from the ER differs in yeast and mammalian cells. *Traffic* **11,** 1017–1033
15. Gazzinelli, R. T., and Denkers, E. Y. (2006) Protozoan encounters with Toll-like receptor signaling pathways: implications for host parasitism. *Nat. Rev. Immunol.* **6,** 895–906
16. Buscaglia, C. A., Campo, V. A., Frasch, A. C., and Di Noia, J. M. (2006) *Trypanosoma cruzi* surface mucins: host-dependent coat diversity. *Nat. Rev. Microbiol.* **4,** 229–236
17. El-Sayed, N. M., Myler, P. J., Blandin, G., Berriman, M., Crabtree, J., Aggarwal, G., Caler, E., Renauld, H., Worthey, E. A., Hertz-Fowler, C., Ghedin, E., Peacock, C., Bartholomeu, D. C., Haas, B. J., Tran, A. N., Wortman, J. R., Alsmark, U. C., Angiuoli, S., Anupama, A., Badger, J., Bringaud, F., Cadag, E., Carlton, J. M., Cerqueira, G. C., Creasy, T., Delcher, A. L., Djikeng, A., Embley, T. M., Hauser, C., Ivens, A. C., Kummerfeld, S. K., Pereira-Leal, J. B., Nilsson, D., Peterson, J., Salzberg, S. L., Shallom, J., Silva, J. C., Sundaram, J., Westenberger, S., White, O., Melville, S. E., Donelson, J. E., Andersson, B., Stuart, K. D., and Hall, N. (2005) Comparative genomics of trypanosomatid parasitic protozoa. *Science* **309,** 404–409
18. Taylor, M. C., and Kelly, J. M. (2006) pTcINDEX: a stable tetracycline-regulated expression vector for *Trypanosoma cruzi*. *BMC Biotechnol.* **6,** 32
19. Stuart, K., Brun, R., Croft, S., Fairlamb, A., Gürtler, R. E., McKerrow, J., Reed, S., and Tarleton, R. (2008) Kinetoplastids: related protozoan pathogens, different diseases. *J. Clin. Invest.* **118,** 1301–1310
20. Previato, J. O., Sola-Penna, M., Agrellos, O. A., Jones, C., Oeltmann, T., Travassos, L. R., and Mendonça-Previato, L. (1998) Biosynthesis of *O*-*N*-acetylglucosamine-linked glycans in *Trypanosoma cruzi*. Characterization of the novel uridine diphospho-*N*-acetylglucosamine:polypeptide *N*-acetylglucosaminyltransferase-catalyzing formation of *N*-acetylglucosamine α1–*O*-threonine. *J. Biol. Chem.* **273,** 14982–14988
21. de Lederkremer, R. M., and Agusti, R. (2009) Glycobiology of *Trypanosoma cruzi*. *Adv Carbohydr. Chem. Biochem.* **62,** 311–366
22. Buscaglia, C. A., Campo, V. A., Di Noia, J. M., Torrecilhas, A. C., De Marchi, C. R., Ferguson, M. A., Frasch, A. C., and Almeida, I. C. (2004) The surface coat of the mammal-dwelling infective trypomastigote stage of *Trypanosoma cruzi* is formed by highly diverse immunogenic mucins. *J. Biol. Chem.* **279,** 15860–15869
23. Yoshida, N. (2006) Molecular basis of mammalian cell invasion by *Trypanosoma cruzi*. *An Acad Bras Cienc* **78,** 87–111
24. Cánepa, G. E., Degese, M. S., Budu, A., Garcia, C. R., and Buscaglia, C. A. (2012) Involvement of TSSA (trypomastigote small surface antigen) in *Trypanosoma cruzi* invasion of mammalian cells. *Biochem. J.* **444,** 211–218
25. Almeida, I. C., Camargo, M. M., Procópio, D. O., Silva, L. S., Mehlert, A., Travassos, L. R., Gazzinelli, R. T., and Ferguson, M. A. (2000) Highly purified glycosylphosphatidylinositols from *Trypanosoma cruzi* are potent proinflammatory agents. *EMBO J.* **19,** 1476–1485
26. Erdmann, H., Steeg, C., Koch-Nolte, F., Fleischer, B., and Jacobs, T. (2009) Sialylated ligands on pathogenic *Trypanosoma cruzi* interact with Siglec-E (sialic acid-binding Ig-like lectin-E). *Cell Microbiol.* **11,** 1600–1611
27. Di Noia, J. M., D'Orso, I., Sánchez, D. O., and Frasch, A. C. (2000) AU-rich elements in the 3′-untranslated region of a new mucin-type gene family of *Trypanosoma cruzi* confers mRNA instability and modulates translation efficiency. *J. Biol. Chem.* **275,** 10218–10227
28. Nakayasu, E. S., Yashunsky, D. V., Nohara, L. L., Torrecilhas, A. C., Nikolaev, A. V., and Almeida, I. C. (2009) GPIomics: global analysis of glycosylphosphatidylinositol-anchored molecules of *Trypanosoma cruzi*. *Mol Syst Biol* **5,** 261
29. Nakayasu, E. S., Sobreira, T. J., Torres, R., Jr., Ganiko, L., Oliveira, P. S., Marques, A. F., and Almeida, I. C. (2012) Improved proteomic approach for the discovery of potential vaccine targets in *Trypanosoma cruzi*. *J. Proteome Res.* **11,** 237–246
30. Urban, I., Santurio, L. B., Chidichimo, A., Yu, H., Chen, X., Mucci, J., Agüero, F., and Buscaglia, C. A. (2011) Molecular diversity of the *Trypanosoma cruzi* TcSMUG family of mucin genes and proteins. *Biochem. J.* **438,** 303–313
31. Campo, V., Di Noia, J. M., Buscaglia, C. A., Agüero, F., Sánchez, D. O., and Frasch, A. C. (2004) Differential accumulation of mutations localized in particular domains of the mucin genes expressed in the vertebrate host stage of *Trypanosoma cruzi*. *Mol. Biochem. Parasitol.* **133,** 81–91
32. Cassola, A., De Gaudenzi, J. G., and Frasch, A. C. (2007) Recruitment of mRNAs to cytoplasmic ribonucleoprotein granules in trypanosomes. *Mol. Microbiol.* **65,** 655–670
33. Vazquez, M. P., and Levin, M. J. (1999) Functional analysis of the intergenic regions of TcP2beta gene loci allowed the construction of an improved *Trypanosoma cruzi* expression vector. *Gene* **239,** 217–225
34. Di Noia, J. M., Sánchez, D. O., and Frasch, A. C. (1995) The protozoan *Trypanosoma cruzi* has a family of genes resembling the mucin genes of mammalian cells. *J. Biol. Chem.* **270,** 24146–24149
35. Labriola, C. A., Conte, I. L., López Medus, M., Parodi, A. J., and Caramelo, J. J. (2010) Endoplasmic reticulum calcium regulates the retrotranslocation of *Trypanosoma cruzi* calreticulin to the cytosol. *PLoS One* **5,** e13141
36. McDowell, M. A., Ransom, D. M., and Bangs, J. D. (1998) Glycosylphosphatidylinositol-dependent secretory transport in *Trypanosoma brucei*. *Biochem. J.* **335,** 681–689
37. Cordero, E. M., Nakayasu, E. S., Gentil, L. G., Yoshida, N., Almeida, I. C., and da Silveira, J. F. (2009) Proteomic analysis of detergent-solubilized membrane proteins from insect-developmental forms of *Trypanosoma cruzi*. *J. Proteome Res.* **8,** 3642–3652
38. Campo, V. A., Buscaglia, C. A., Di Noia, J. M., and Frasch, A. C. (2006) Immunocharacterization of the mucin-type proteins from the intracellular stage of *Trypanosoma cruzi*. *Microbes Infect.* **8,** 401–409
39. Pitcovsky, T. A., Buscaglia, C. A., Mucci, J., and Campetella, O. (2002) A functional network of intramolecular cross-reacting epitopes delays the elicitation of neutralizing antibodies to *Trypanosoma cruzi* trans-sialidase. *J. Infect. Dis.* **186,** 397–404
40. Yu, H., Chokhawala, H., Karpel, R., Yu, H., Wu, B., Zhang, J., Zhang, Y., Jia, Q., and Chen, X. (2005) A multifunctional Pasteurella multocida sialyltransferase: a powerful tool for the synthesis of sialoside libraries. *J. Am. Chem. Soc.* **127,** 17618–17619
41. Field, M. C., Moran, P., Li, W., Keller, G. A., and Caras, I. W. (1994) Retention and degradation of proteins containing an uncleaved glycosylphosphatidylinositol signal. *J. Biol. Chem.* **269,** 10830–10837
42. Heske, J., Heller, U., Winklhofer, K. F., and Tatzelt, J. (2004) The C-terminal globular domain of the prion protein is necessary and sufficient for import into the endoplasmic reticulum. *J. Biol. Chem.* **279,** 5435–5443
43. He, C. Y., Pypaert, M., and Warren, G. (2005) Golgi duplication in *Trypanosoma brucei* requires Centrin2. *Science* **310,** 1196–1198
44. Bütikofer, P., Malherbe, T., Boschung, M., and Roditi, I. (2001) GPI-anchored proteins: now you see 'em, now you don't. *Faseb J.* **15,** 545–548
45. Schenkman, S., Ferguson, M. A., Heise, N., de Almeida, M. L., Mortara, R. A., and Yoshida, N. (1993) Mucin-like glycoproteins linked to the membrane by glycosylphosphatidylinositol anchor are the major acceptors of sialic acid in a reaction catalyzed by trans-sialidase in metacyclic forms of

Trypanosoma cruzi. *Mol. Biochem. Parasitol.* **59,** 293–303
46. Di Noia, J. M., Buscaglia, C. A., De Marchi, C. R., Almeida, I. C., and Frasch, A. C. (2002) A *Trypanosoma cruzi* small surface molecule provides the first immunological evidence that Chagas' disease is due to a single parasite lineage. *J. Exp. Med.* **195,** 401–413
47. Böhme, U., and Cross, G. A. (2002) Mutational analysis of the variant surface glycoprotein GPI-anchor signal sequence in *Trypanosoma brucei*. *J. Cell Sci.* **115,** 805–816
48. Stewart, M. (2007) Molecular mechanism of the nuclear protein import cycle. *Nat. Rev. Mol. Cell Biol.* **8,** 195–208
49. Ferella, M., Nilsson, D., Darban, H., Rodrigues, C., Bontempi, E. J., Docampo, R., and Andersson, B. (2008) Proteomics in *Trypanosoma cruzi*–localization of novel proteins to various organelles. *Proteomics* **8,** 2735–2749
50. Pollevick, G. D., Di Noia, J. M., Salto, M. L., Lima, C., Leguizamón, M. S., de Lederkremer, R. M., and Frasch, A. C. (2000) *Trypanosoma cruzi* surface mucins with exposed variant epitopes. *J. Biol. Chem.* **275,** 27671–27680
51. Macrae, J. I., Acosta-Serrano, A., Morrice, N. A., Mehlert, A., and Ferguson, M. A. (2005) Structural characterization of NETNES, a novel glycoconjugate in *Trypanosoma cruzi* epimastigotes. *J. Biol. Chem.* **280,** 12201–12211
52. Hollingsworth, M. A., and Swanson, B. J. (2004) Mucins in cancer: protection and control of the cell surface. *Nat. Rev. Cancer* **4,** 45–60
53. Bangs, J. D., Ransom, D. M., McDowell, M. A., and Brouch, E. M. (1997) Expression of bloodstream variant surface glycoproteins in procyclic stage *Trypanosoma brucei*: role of GPI anchors in secretion. *EMBO J.* **16,** 4285–4294
54. Schwartz, K. J., Peck, R. F., Tazeh, N. N., and Bangs, J. D. (2005) GPI valence and the fate of secretory membrane proteins in African trypanosomes. *J. Cell Sci.* **118,** 5499–5511
55. McGwire, B. S., and Chang, K. P. (1996) Posttranslational regulation of a Leishmania HEXXH metalloprotease (gp63). The effects of site-specific mutagenesis of catalytic, zinc binding, *N*-glycosylation, and glycosyl phosphatidylinositol addition sites on N-terminal end cleavage, intracellular stability, and extracellular exit. *J. Biol. Chem.* **271,** 7903–7909
56. McGwire, B. S., O'Connell, W. A., Chang, K. P., and Engman, D. M. (2002) Extracellular release of the glycosylphosphatidylinositol (GPI)-linked Leishmania surface metalloprotease, gp63, is independent of GPI phospholipolysis: implications for parasite virulence. *J. Biol. Chem.* **277,** 8802–8809
57. Ralton, J. E., Mullin, K. A., and McConville, M. J. (2002) Intracellular trafficking of glycosylphosphatidylinositol (GPI)-anchored proteins and free GPIs in *Leishmania mexicana*. *Biochem. J.* **363,** 365–375
58. Di Noia, J. M., D'Orso, I., Aslund, L., Sánchez, D. O., and Frasch, A. C. (1998) The *Trypanosoma cruzi* mucin family is transcribed from hundreds of genes having hypervariable regions. *J. Biol. Chem.* **273,** 10843–10850